PHYSICAL REVIEW A **80**, 021601(R) (2009)

# Vortex-induced phase-slip dissipation in a toroidal Bose-Einstein condensate flowing through a barrier

F. Piazza,[1] L. A. Collins,[2] and A. Smerzi[1]
[1]*Dipartimento di Fisica and CNR–INFM BEC Center, Università di Trento, I-38050 Povo, Italy*
[2]*Theoretical Division, Los Alamos National Laboratory, Mail Stop B214, Los Alamos, New Mexico 87545, USA*
(Received 3 March 2009; published 10 August 2009)

We study superfluid dissipation due to phase slips for a Bose-Einstein condensate flowing through a repulsive barrier inside a torus. The barrier is adiabatically raised across the annulus, while the condensate flows with a finite quantized angular momentum. At a critical height, a vortex moves from the inner region and reaches the barrier to eventually circulate around the annulus. At a higher critical height, an antivortex also enters into the torus from the outer region. Both vortex and antivortex decrease the total angular momentum by leaving behind a $2\pi$ phase slip. When they collide and annihilate or orbit along the same loop, the condensate suffers a global $2\pi$ phase slip, and the total angular momentum decreases by one quantum. In hydrodynamic regime, the instability sets in when the local superfluid velocity equals the sound speed inside the barrier region.

DOI: 10.1103/PhysRevA.80.021601 PACS number(s): 03.75.Kk, 03.75.Lm, 47.32.−y

## I. INTRODUCTION

Flow dynamics through a constriction can reveal essential aspects of superfluidity. A central feature observed long ago with superfluid $^4$He currents through an orifice [1] is the occurrence of single $2\pi$ phase slips, which collectively decrease the fluid velocity by a quantized amount. More recently, the transition from phase slips to the Josephson regime has been observed by increasing the helium healing length with respect to the size of the orifice [2].

Common belief associates phase slips with the nucleation of vortices transversally crossing the constriction [3]. This mechanism has been invoked to explain the dissipation of the superfluid helium flow, which occurs at critical velocities much lower than predicted by the Landau criterion. The microscopic mechanism of the onset of the instability and its dynamical evolution, however, are still not completely understood [4].

The superflow dynamics of a dilute Bose-Einstein condensate (BEC) gas can shed light on the physics of phase slips. While in quantum liquids constrictions are made by single or multiple orifices, in BECs they can be created by a laser beam generating a repulsive barrier for the atoms or by an offset of the central hole in toroidal geometries [5]. Broadly speaking, similar configurations allow for the observation of macroscopic phase coherence effects and can lead to a range of important technologies. While superconducting Josephson junctions are already employed in sensors and detectors, their superfluid counterparts can realize ultrasensitive gyroscopes to detect rotations [2]. For instance, a toroidally shaped superfluid weak link provides the building block of a dc superconducting quantum interference device (SQUID), which is the most promising sensing device based on superfluid interference.

A distinctive feature of quantum gases rests with the possibility of experimentally interrogating the response of the system in a wide variety of traps and dynamical configurations. Moreover, even if the BEC is described by a local Gross-Pitaevskii Eq. (GPE) (1) (as in most cases where dipolar interactions can be neglected) and therefore lacks the rotonic part of the helium spectrum, its nonlinearity appears to be the only crucial ingredient needed to reveal the microscopic mechanisms underlying the vortex-induced phase slips. Superfluidity of a BEC confined in a torus, in absence of barriers, has been first experimentally observed at NIST [5]. The BEC was initially stirred by transfer of quantized orbital angular momentum from a Laguerre-Gaussian beam and the rotation remained stable up to 10 s in the multiply connected trap. The metastability of a ring-shaped superflow due to centrifugal forces has been observed in [6]. The superfluid critical velocity in a harmonically trapped BEC swept by a laser beam has been observed experimentally in [7] and associated with the creation of vortex phase singularities in [8], while solitons were observed in the one-dimensional geometry of [9]. Such problems have been object of a large theoretical study mainly based on numerical simulations of the GPE [10].

In this Rapid Communication, we theoretically study the dynamics of a BEC flowing inside a toroidal trap at zero temperature and in the presence of a repulsive barrier. Similar qualitative results are observed when, rather than by a repulsive barrier, the constriction is created by an offset in the position of the central hole of the torus. As initial condition, we consider a superfluid state with a finite orbital angular momentum in the cylindrically symmetric torus. The critical regime is reached by adiabatically raising the standing repulsive barrier. The dissipation takes place through phase slips created by singly-quantized vortex lines crossing the flow. We found two different critical barrier heights. At the smallest critical height, a singly-quantized vortex moves radially along a straight path from the center of the torus and enters the annulus [Figs. 1(a) and 1(b)], leaving behind a $2\pi$ phase slip. Eventually, it keeps circulating with the background flow without crossing completely the torus so that it decreases the total angular momentum only by a fraction of unity. At the highest critical height, a singly-quantized

 

RAPID COMMUNICATIONS



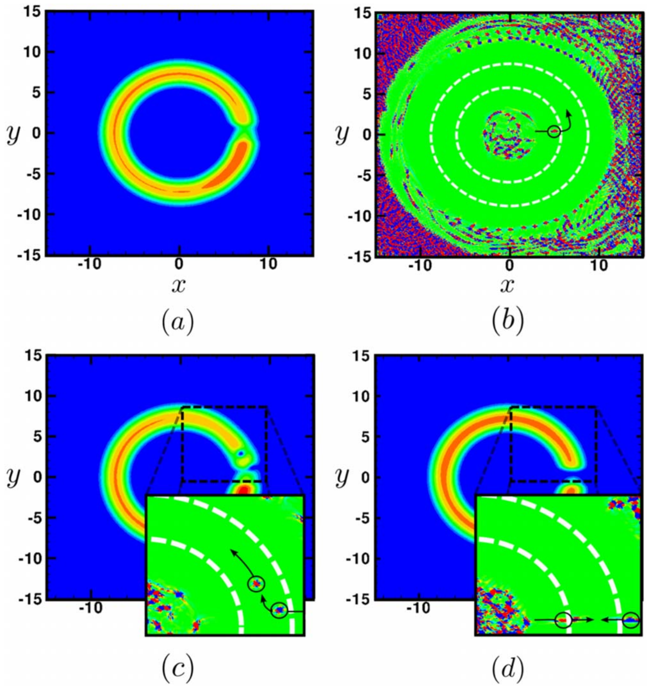

FIG. 1. (Color online) [(a)–(c)] $t_r=10$, $L_z/N=8$, and $V_s=0.34\ \mu$. (a) $t=7.6$. Density contour plot with no visible vortex core. (b) $t=7.6$. The $z$ component of the vorticity field $\nu(\mathbf{r})$. The white dashed lines indicates the TF radii of the cloud. The encircled dot corresponds to a vortex about to enter the annulus from the inner edge. (c) $t=11.6$. A vortex circulates along the annulus while the vorticity (inset) shows an antivortex about to enter. (d) $t_r=10$, $L_z/N=2$, and $V_s=0.61\ \mu$. Vortex antivortex annihilation.

antivortex enters the torus from the outward low-density region of the system. The ensuing vortex dynamics depends on the velocity asymmetry between the inner and the outer edge of the annulus as well as on the final barrier height and ramping time. For instance, a vortex and an antivortex can just circulate on separate orbits [Fig. 1(c)] or can collide along a radial trajectory and annihilate [Fig. 1(d)]. When they orbit on the same loop or annihilate, the system undergoes a global $2\pi$ phase slip, with the decrease of one unit of total angular momentum. In general, the BEC flow can be stabilized after the penetration of a few vortices.

In hydrodynamic regime, we find that the instability toward vortex penetration occurs when the local superfluid velocity equals the sound speed. This happens inside the barrier region and close to the edges of the cloud. We have studied the above scenario in two-dimensional (2D) and three-dimensional (3D) numerical simulations of the dynamical GPE. In the 3D analysis, we have employed the experimental parameters of the toroidal trap created at NIST [11]. The experimental investigation of the system proposed here can provide the first direct observation of interconnection and dynamical evolution of vortices and phase slips in superfluid systems.

## II. PHASE-SLIPS AND VORTICES

We numerically solve the time-dependent GPE

$$i\hbar\frac{\partial\psi(\boldsymbol{r},t)}{\partial t}=\left[-\frac{\hbar^2\nabla^2}{2m}+V_t(\boldsymbol{r})+V_b(\boldsymbol{r},t)+g|\psi|^2\right]\psi(\boldsymbol{r},t), \quad (1)$$

where $g$ is proportional to the interparticle scattering length. In the following, we first consider an effective 2D Cartesian geometry [12] and eventually extend the analysis to the 3D configuration. The trapping potential $V_t(\boldsymbol{r})=V_h(\boldsymbol{r})+V_c(\boldsymbol{r})$ is made by an harmonic confinement $V_h(\boldsymbol{r})=\hbar\omega_\perp(x^2+y^2)/2d_\perp^2$ plus a Gaussian core $V_c(\boldsymbol{r})=V_0\exp[-(x^2+y^2)/\sigma_c^2]$ creating a hole in the trap center (in what follows we will express quantities in trap units of time $\omega_\perp^{-1}$ and length $d_\perp$). As an initial condition, we consider the numerical ground state obtained with $V_b=0$ and transfer by linear phase imprinting (in 3D calculations a Laguerre-Gaussian beam is implemented [11]) a total angular momentum $L_z=Nl$, with $N$ as the total number of particles and $l$ as an integer. The transferred angular momentum is low enough to have flow velocities in the torus region much smaller than the sound speed. Over each loop of radius $r=\sqrt{x^2+y^2}$ the circulation is $C=2\pi l$ and the modulus of the fluid velocity, $v(r)=C/2\pi r$, is constant and directed along the tangent of the same loop. In principle, these $l$ quanta of circulation can be carried by a single multiply quantized macrovortex [13], which however breaks up into singly-quantized vortices still confined within the central hole [14]. In our simulations, as soon as a finite angular momentum is transferred to the condensate, the vorticity field component perpendicular to the $x$-$y$ plane $\nu(\boldsymbol{r},t)=[\boldsymbol{\nabla}\times\boldsymbol{v}(\boldsymbol{r},t)]\cdot\hat{z}$ shows a "sea" of positive and negative vorticity spots, that is, a mesh of vortices and antivortices [Fig. 1(b)]. This happens in two regions of very low density, close to the center and in the space surrounding the torus [15].

After angular momentum is transferred to the cloud, the barrier potential $V_b(\boldsymbol{r},t)$ is slowly ramped up over a time $t_r$ to a final height $V_s$. We use a repulsive well with widths $w_x$ centered at the maximum density and $w_y$ centered at $y=0$ [16]. We always choose $w_x>d$, where $d\equiv R_2-R_1$ is the width of the annulus. Initially, the density and velocity field adapt to the presence of the barrier, and the flow shows no sign of dissipation. In the barrier region, where the density is depleted, the flow velocity increases mainly at the edges of the annulus. By examining the vorticity, we observe that the two vortex seas are strongly fluctuating, with vortices and antivortices trying to escape but being pushed back by zones of higher density. However, when the barrier reaches a critical height $V_{c1}$, a vortex from the inner sea can successfully escape and enter the annulus. As shown in Figs. 1(a) and 1(b) [17], at $V_{c1}$ the flow can no longer sustain a stationary configuration and becomes unstable. In Fig. 1(a), we observe the depletion of the density but not a visible vortex core. However, if we inspect the vorticity field plotted in Fig. 1(b), we clearly see an isolated red spot, corresponding to a positive vorticity, moving radially from the center of the torus toward the higher density region, indicating the presence of the core of a singly-quantized vortex [18].

The above scenario for vortex nucleation in a multiply connected geometry confirms that a persistent flow in such a configuration is possible because of the pinning of the vorticity in the low-density regions near the center and outside of the torus. The pinning is due to the effective energy bar-

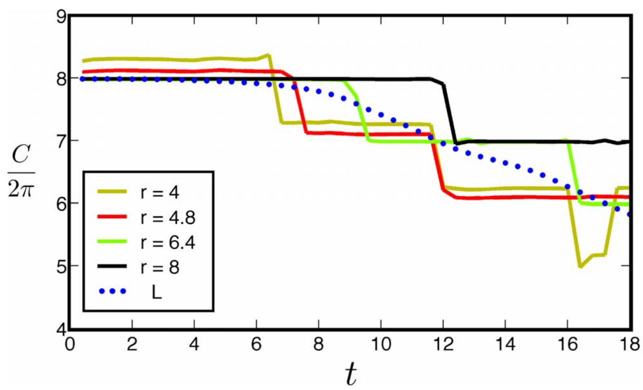


FIG. 2. (Color online) Circulation (solid lines) for loops with different radii and total angular momentum (dots) as a function of time. The parameters are the same as in Fig. 1(a). The $2\pi$ drops in the circulation at $r=4,4.8,6.4$ are due to a singly-quantized vortex moving outwards from the center. The drop at $r=8$ and $t\sim 12$ is due to the passage of an antivortex entering the annulus from the outer edge. The oscillation in the circulation at $r=4$ and $t\sim 16-17$ is due to a double crossing of a vortex trying to escape the inner region.

rier felt from a vortex core when trying to move toward a region of much higher density [19]. The effective energy barrier arises from the nonlinearity of the GPE. The obstacle raised across the annulus serves to unpin singly-quantized vortices by steadily decreasing the density during the ramping process, up to suppression of the effective energy barrier. The density depletion occurs on a radial stripe and makes way for the vortex moving outwards along a straight line connecting the center of the vortex with the barrier. This as well happens for the antivortex moving inwards at a larger height of the repulsive barrier, see below.

In the hydrodynamic regime, when $\xi \ll d, w_x, w_y$ and $V_s \ll \mu$, we observe the instability toward vortex penetration when the local superfluid velocity reaches the sound speed [20]. This sound speed, which depends on the density integrated along the radial direction [13], is calculated along a line at the maximum of the repulsive well (at $y=0$ in our case). The critical condition is first met inside the barrier region where the density is depleted, at a position very close to the Thomas-Fermi radius of the cloud. The parameters of Fig. 1, however, have been chosen such that the system is outside the hydrodynamic regime, in order to emphasize the generality of the presented vortex dynamics phenomenology [21].

The passage of a vortex core between two points causes a $2\pi$ slip in the phase difference between them [3]. In Fig. 2, we observe $2\pi$ sharp drops in the circulation $C$ on a given loop of radius $r$ at the moment the vortex core crosses it. Moreover, at small radii, close to the inner sea of vortices, the circulation shows spikes at which it decreases by $2\pi$, then quickly goes back to its previous value. These are associated with a vortex moving out of the sea but being pushed back by a region of high density located slightly outwards, as discussed above.

Due to phase slippage, the angular momentum is reduced, and eventually the system becomes stable again after a finite number of spawned vortices. The circulation is lowered by a few quanta, and the fluid velocity on vortex-crossed loops is brought back below the critical value. If the ramping is stopped at $V_{c1}$, only the inner edge of the annulus is unstable since its fluid velocity is larger ($v(r) \propto l/r$). In this case, vortices do not cross completely the torus and move on stable circular orbits [22].

However, when the barrier reaches a second critical height $V_{c2} > V_{c1}$ the outer part of the annulus becomes also unstable. Antivortices then enter from outwards while vortices enter the inner edge, as previously discussed. Antivortices move radially inwards and contribute to stabilize the outer part by phase slips. Indeed, an antivortex crossing a loop makes the circulation drop as a vortex crossing the opposite way. In Fig. 1(c) we see a vortex already circulating inside the high-density region of the annulus while an antivortex begins to enter. The separation between $V_{c1}$ and $V_{c2}$ is proportional to the velocity difference $\Delta v = l(R_1 - R_2)/(R_1 R_2)$ between the two edges. In general, depending on $\Delta v$, the dynamics at barrier heights larger than $V_{c2}$ can vary. For instance, at lower angular momenta $\Delta v$ becomes smaller, and a vortex and an antivortex enter the annulus almost simultaneously. They can then collide and annihilate, as shown in Fig. 1(d). When a vortex and an antivortex annihilate or separately orbit on the same loop, the system undergoes a global $2\pi$ phase slip, and the total angular momentum is decreased by one unit.

We extend our 2D calculations into a 3D configuration [23]. The parameters of the toroidal trap are those employed experimentally at NIST [11]. We add a repulsive well potential [16] whose shape, however, is not crucial in determining the qualitative features of the dissipation as long as $w_x$ is larger than the width of the annulus. We found that the nucleation of singly-quantized vortex lines and their dynamics resemble those observed in 2D calculations. In particular, we have two critical values for the barrier height $V_{c1}$ and $V_{c2}$ connected, respectively, with the nucleation of vortices or both vortices and antivortices.

## III. CONCLUSIONS

We have studied the superfluid dynamics of a dilute Bose-Einstein condensate confined in a toroidal trap in presence of a repulsive barrier. With a finite initial angular momentum, we observed two critical values of the barrier height for the onset of phase slips dissipation: a lower one corresponding to vortices entering the annulus from the center of the torus, and a higher one related to both vortices and antivortices, the latter entering the outer edge of the annulus. We have performed 3D simulations with the NIST toroidal trap parameters, where the above scenario could be experimentally observed when a standing repulsive barrier is raised across the BEC supefluid flow. Since supercurrents have recently been observed in absence of the barrier, we believe that the experimental confirmation of our results is at hand. Vortices can be directly observed with BECs, and it is therefore possible to experimentally characterize their role in phase-slip-induced dissipation in superfluid systems.

## ACKNOWLEDGMENTS

We would like to thank B. Schneider, F. Dalfovo, L. Pitaevskii, and S. Stringari for helpful discussions and Dr. S. Hu for assistance with the 3D GPE program. We acknowledge useful exchanges with W. Phillips, S. Muniz, A. Ramanathan, K. Helmerson, and P. Clade. The Los Alamos National Laboratory is operated by Los Alamos National Security, LLC for the National Nuclear Security Administration of the (U.S.) Department of Energy under Contract No. DE-AC52-06NA25396.

[1] O. Avenel and E. Varoquaux, Phys. Rev. Lett. **55**, 2704 (1985).
[2] E. Hoskinson, Y. Sato, I. Hahn, and R. E. Packard, Nat. Phys. **2**, 23 (2006).
[3] P. W. Anderson, Rev. Mod. Phys. **38**, 298 (1966).
[4] R. E. Packard, Rev. Mod. Phys. **70**, 641 (1998); É. Varoquaux, C. R. Phys. **7**, 1101 (2006).
[5] C. Ryu *et al.*, Phys. Rev. Lett. **99**, 260401 (2007).
[6] P. Engels, I. Coddington, P. C. Haljan, V. Schweikhard, and E. A. Cornell, Phys. Rev. Lett. **90**, 170405 (2003).
[7] C. Raman *et al.*, Phys. Rev. Lett. **83**, 2502 (1999); R. Onofrio *et al.*, *ibid.* **85**, 2228 (2000).
[8] S. Inouye *et al.*, Phys. Rev. Lett. **87**, 080402 (2001).
[9] P. Engels and C. Atherton, Phys. Rev. Lett. **99**, 160405 (2007).
[10] T. Frisch, Y. Pomeau, and S. Rica, Phys. Rev. Lett. **69**, 1644 (1992); M. Stone and A. M. Srivastava, J. Low Temp. Phys. **102**, 445 (1996); B. Jackson, J. F. McCann, and C. S. Adams, Phys. Rev. Lett. **80**, 3903 (1998); A. Aftalion, Q. Du, and Y. Pomeau, *ibid.* **91**, 090407 (2003); C. T. Pham, C. Nore, and M. E. Brachet, Physica D **210**, 203 (2005); V. Hakim, Phys. Rev. E **55**, 2835 (1997); N. Pavloff, Phys. Rev. A **66**, 013610 (2002); I. Carusotto, S. X. Hu, L. A. Collins, and A. Smerzi, Phys. Rev. Lett. **97**, 260403 (2006); M. Albert, T. Paul, N. Pavloff, and P. Leboeuf, *ibid.* **100**, 250405 (2008).G. Watanabe, F. Dalfovo, F. Piazza, L. P. Pitaevskii, and S. Stringari e-print arXiv:0907.0621.
[11] W. D. Phillips (private communications); We use an harmonic trapping with $\omega_\perp=2\pi\times 20$ Hz (such that $d_\perp=4.69$ $\mu$m) and $\omega_z=48\omega_\perp$. The Laguerre-Gaussian beam is modeled by a proper external potential term in the GPE, see T. P. Simula *et al.*, Phys. Rev. A **77**, 015401 (2008).
[12] We solved the 2D GPE numerically by a finite-difference real-space product formula (RSPF) approach and employed a spatial grid of 300–600 points extending from −15 to +15 in both the $x$ and $y$ directions with a time step of $1\times 10^{-5}$ (quantities given in trap units, see text below); see L. Collins *et al.*, Comput. Phys. Commun. **114**, 15 (1998) for details.
[13] M. Cozzini, B. Jackson, and S. Stringari, Phys. Rev. A **73**, 013603 (2006).
[14] A. Aftalion and I. Danaila, Phys. Rev. A **69**, 033608 (2004).
[15] We can regard the presence of the "vortex sea" as due to numerical noise acting inside very low-density regions, possibly triggering a dynamical instability of GPE.
[16] The barrier potential is $V_b(\boldsymbol{r},t)=f(t)V_sV_{bx}(x)V_{by}(y)/4$, with $f(t)=t/t_r$ [$f(t)=1$ for $t>t_r$] and $V_{bx}=\tanh[(x-R_x+x_0)/b_s]+\tanh[(-x+R_x+x_0)/b_s]$. Here $R_x$ is the $x$ shift of the center of the barrier while its width is $w_x\sim 2x_0$. $V_{by}$ has the same shape as $V_{bx}$ but with $R_y=0$. The final height of the barrier is $V_s$ as long as $x_0,y_0 \gg b_s$.
[17] Before raising the barrier, the flow velocity at the maximum density, located at $r_m=7.2$, is $v(r_m)=0.67\ c_s$, where $c_s$ is Thomas-Fermi (TF) estimate of the sound speed in the ground state. The TF value of the healing length at $r_m$ is $\xi\sim 0.28$. The TF width of the annulus is $d=3.59$. In this case, the barrier widths are $w_x\sim 4$ and $w_y\sim 2$. The observed critical barrier heights are $V_{c1}\sim 0.14\ \mu$ and $V_{c2}\sim 0.24\ \mu$.
[18] In the literature, phase singularities appearing inside strongly depleted regions have been referred to as "ghost vortices," see M. Tsubota, K. Kasamatsu, and M. Ueda, Phys. Rev. A **65**, 023603 (2002).
[19] Experimentally observed in S. Tung, V. Schweikhard, and E. A. Cornell, Phys. Rev. Lett. **97**, 240402 (2006) with optical lattices. For toroidal superfluid is theoretically studied in J. Tempere, J. T. Devreese, and E. R. I. Abraham, Phys. Rev. A **64**, 023603 (2001); F. Bloch, *ibid.* **7**, 2187 (1973); A. J. Leggett, Rev. Mod. Phys. **73**, 307 (2001); M. Benakli *et al.*, Europhys. Lett. **46**, 275 (1999).
[20] In hydrodynamics, instabilities appear in the flow past a finite body as soon as the velocity becomes supersonic at some point, L. D. Landau and E. M. Lifshitz, *Fluid Mechanics*, 2nd English ed. (Pergamon Press, New York, 1987). In the case of a BEC in hydrodynamic regime this has been verified for instance in one-dimensional flows through a penetrable barrier and also in the case of a two-dimensional flow past an impenetrable disk, see [10].
[21] Indeed, the critical barrier heights $V_{c1}=0.14\ \mu$ and $V_{c2}=0.24\ \mu$, determined from simulations, are different from $V_{c1}=0.08\ \mu$ and $V_{c2}=0.17\ \mu$ which we predict analytically using the hydrodynamic condition for instability. These critical heights are determined using the GPE stationary solutions in TF approximation. F. Piazza, L. A. Collins, and A. Smerzi (to be published).
[22] The vortices circulate on a fixed loop within our computational times. Vortices orbiting inside a 2D toroidal trap have been studied with GPE, see P. Mason and N. G. Berloff, Phys. Rev. A **79**, 043620 (2009); J.-P. Martikainen, K. A. Suominen, L. Santos, T. Schulte, and A. Sanpera, *ibid.* **64**, 063602 (2001).
[23] We solve the 3D GPE numerically by a finite-element discrete variable representation in the spatial coordinates and a RSPF in time. The $x$ and $y$ coordinates were divided into boxes of span [−20.0,+20.0] with 160 elements and order 5 Gauss-Legendre bases while the $z$ direction covered a box [−10.0, +10.0] with 80 elements of order 5 bases. The time step was $1\times 10^{-5}$ see B. I. Schneider, L. A. Collins, and S. X. Hu, Phys. Rev. E **73**, 036708 (2006) for details.